Int. J. Electrochem. Sci., 9 **(2014)** 810 - 820

International Journal of
ELECTROCHEMICAL
SCIENCE
www.electrochemsci.org

Production of Graphene by Liquid-Phase Exfoliation of Intercalated Graphite

Ming Zhou,[1] *Tian Tian,*[1] *Xuanfu Li,*[1,2] *Xudong Sun,*[1] *Juan Zhang,*[1,2] *Ping Cui,*[1] *Jie Tang,*[3] *and Lu-Chang Qin*[1,4]

[1]Division of Functional Materials and Nano-Devices, Ningbo Institute of Materials Technology and Engineering, Chinese Academy of Sciences, Ningbo 315201, China
[2]School of Materials Science and Chemical Engineering, Ningbo University, Ningbo 315201, China
[3]National Institute for Materials Sciences, Tsukuba 305-0047, Japan
[4]Department of Physics and Astronomy, University of North Carolina at Chapel Hill, Chapel Hill, NC 27599-3255, USA
*E-mail: lcqin@email.unc.edu

Received: 14 May 2013 / *Accepted:* 2 November 2013 / *Published:* 8 December 2013

Liquid-phase exfoliation of tetraethylammonium graphite intercalation compound (TEA-GIC) has been prepared by high-power tip-sonication of graphite in aqueous TEA solution. The release of gaseous species due to the decomposition of TEA under microwave irradiation led to huge expansion of graphite. The expanded graphite was then exfoliated to produce graphene under mild sonication in organic solvents. Raman and X-ray photoelectron spectroscopy measurements indicated that the thus prepared graphene had few defects and little oxidation. In addition, the graphene films exhibited an electrical conductivity of 5000 S m^{-1} and the production process is easy to scale up and the single-cycle yield reached is as high as 5%.

Keywords: graphene, graphite, exfoliation, intercalation

1. INTRODUCTION

Graphene has attracted great interests during the past decade [1-3]. The excellent electrical and optical properties make it promising in a variety of devices such as high speed transistors [4-6], transparent conducing films [7,8], lithium ion batteries [9-11], and supercapacitors [9,11,12]. Its electrical conductivity, which is largely affected by the presence of defects and functional groups, governs the performance of many of these devices [13]. Therefore, the preparation of graphene with

low concentration of defects and functional groups is crucial for many of its applications. In addition, in view of industrial applications, high-yield production is also highly demanded.

Liquid-phase exfoliation has been considered as one of the most feasible approach for industrial production of graphene due to its scalability and low cost. This approach typically involves sonication of graphite or graphite oxide powders in solvents. Depending on the graphite precursors, liquid-phase exfoliation of graphite has been studied using (1) graphite oxide, (2) natural graphite, and (3) graphite intercalation compound (GIC).

Liquid-phase exfoliation of graphite oxide is now one of the most widely used methods for preparation of graphene. This method begins with intercalation of graphite with strong oxidizing agents followed by expansion of graphite layers via sonication. The reduction of the obtained graphene oxide to graphene is usually conducted by either thermal or chemical approaches [14,15]. Although this method is capable of high-yield (>50%) production of graphene, the use of large quantity of acid and oxidizing agents requires time-consuming washing steps and produces hazardous wastes. In addition, the vigorous oxidation of graphite often leads to incomplete restoration of the sp^2 hybrid carbon bonds and presence of residual oxygen functional groups resulting in poor electrical conductance [16].

Liquid phase exfoliation of natural graphite is easy to implement and can circumvent the oxidation of graphene. This method involves ultrasonic treatment of graphite in solvents such as N-methyl-2-pyrrolidone (NMP), N'N-dimethylformamide (DMF), and γ-butyrolactone (GBL) [17]. Among all the solvents, NMP gives the highest graphene yield due to its surface energy approaching that of graphite that is sufficient to overcome the interacting forces between graphene layers. Although technically it is similar to the liquid-phase exfoliation of graphite oxide, this method is unique with the absence of oxidative intercalation steps. Graphene prepared by this method was demonstrated to have low concentration of defects and oxygen functional groups. However, the yield is usually very low (~1 wt%) as only the surface layers of graphite were peeled off during sonication.

Liquid-phase exfoliation of GICs for production of graphene was first reported by Viculis et al and has attracted great interest recently [18-21]. This method begins with intercalation of graphite followed by expansion of graphite via rapid increase in the vapor pressure of the volatile intercalated substance under microwave or thermal treatment. As nonoxidative agents are applied for intercalation of graphite and microwave or thermal treatment of GIC leads to large expansion of graphite, high-yield production of graphene with high quality can be achieved using this method. For example, it was reported that, by solvothermal-assisted exfoliation of expanded graphite (EG) obtained from GIC in acetonitrile, Qian et al. successfully prepared mololayer and bilayer graphene with 10-12 wt% yield without significant structural defects [22]. However, these recipes are limited by using either poisonous chemical agents [19] or dangerous chemical reactions [20,21].

In this paper we report liquid-phase exfoliation to produce graphene from tetraethylammonium graphite intercalation compound (TEA-GIC). The intercalation of nontoxic TEA was achieved by simple high-power tip-sonication of graphite in TEA aqueous solution. The release of gaseous species due to the decomposition of TEA under microwave irradiation facilitates the expansion of graphite layers. Graphene were obtained by mild sonication of the expanded graphite in NMP. The obtained

graphene is also characterized by both microscopy and spectroscopy techniques to understand the nanoscale structure and mechanisms of formation responsible for the production processes.

2. EXPERIMENTAL

2.1. Preparation of graphene

Natural graphite (2 g, 99.99% purity) was first mixed with an aqueous solution (300 ml) containing TEA tetrafluoroborate (0.8 g), sodium hydroxide (0.15 g), and thionin acetate salt (50 mg). After agitation for 10 minutes, the suspension was tip sonicated for 6 hours (Scientz-II D Ultrasonic Cell Disruptor, 950 W, with 90% amplitude modulation) and then vacuum filtered by Nylon membrane of 220 nm in pore size. The obtained TEA-GIC was washed with 20 ml deionized water and 20 ml ethanol for three times successively and then vacuum dried at 60 °C for 2 hours. After that, the dry graphite powders were microwave irradiated for 5 minutes (Midea microwave oven, 900 W). The expanded graphite (EG) obtained by microwave treatment was then treated ultrasonically in 700 ml NMP for 2 hours (Ultrasonic Cleaner, 250 W). The resultant suspension containing graphene was centrifuged at 5000 rpm for 15 minutes to remove unexfoliated graphite particles. A stable graphene suspension was obtained finally after the supernatant was pipetted off.

2.2. Preparation of graphene films

100 ml graphene NMP dispersion with a concentration of 0.14 mg ml^{-1} was filtered by Nylon membrane with 220 nm in pore size. The obtained thin graphene paper was dried at 60 °C for 36 hours.

2.3. Structural characterization

The morphology of natural graphite, TEA-GIC, EG, and graphene films was examined by field-emission scanning electron microscopy (SEM, Hitachi S-4800). Atomic force microscope (AFM) characterization was conducted with a Veeco Dimension 3100V scanning probe microscope at ambient conditions using the tapping mode. The sample for AFM measurement was prepared by dip-coating. A mica sheet was immersed in 0.001 mg ml^{-1} graphene NMP dispersion for 5 minutes to adsorb a thin layer of graphene flakes. After that, it was immersed in de-ionized water for another 5 minutes to remove unadsorbed graphene. Powder X-ray diffraction (XRD) patterns of natural graphite, TEA-GIC, and EG were recorded with Bruker AXS D8 Advanced X-Ray Diffractometer. The electrical conductivity of graphene film was measured by a physical property measurement system (PPMS) (Quantum Design Model-9). The structural information of natural graphite, TEA-GIC, and EG was also obtained from Fourier transform infrared spectra (FTIR), which were acquired using a Thermal Nicolet 6700 FTIR spectrometer. Raman and X-ray photoelectron spectroscopy (XPS) measurements were carried out using a Raman microscope (Thermo Scientific DXR) with 532 nm laser and Multifunctional XPS (Shimadzu Axis Utltradld), respectively.

3. RESULTS AND DISCUSSION

3.1. Preparation of graphene

The process of preparing graphene consisted of three steps, as shown schematically in Figure 1: (a) aqueous phase intercalation of natural graphite to produce TEA-GIC, (b) microwave irradiation to obtain EG, and (c) sonication of EG in organic solvents such as NMP, DMF and GBL to obtain graphene. The TEA-GIC was produced by tip sonication (855 W) of graphite in aqueous solution containing thionin acetate salt, sodium hydroxide and TEA. Thionin cations entered graphite galleries after the intercalation of TEA to stabilize TEA-GIC while sodium hydroxide provided hydroxide anions for subsequent elimination of TEA. The TEA-GIC was further microwave irradiated in air. The release of gaseous species induced by the decomposition of TEA led to expansion of graphite. After mild sonication in organic solvent, this EG could be readily exfoliated into dispersive graphene sheets. The single-cycle yield of graphene was 5% determined by weighing the residue after filtration of the graphene dispersion. This value is four times higher than that obtained by liquid-phase exfoliation of graphite in NMP for half an hour [17] and even higher than that obtained by treatment of graphite using the same method for 460 hours [23]. The yield of graphene can be further improved with unexfoliated graphite recycled to repeat the above process.

We observed the Tyndall effect with a laser passing through the dispersion, indicating that the graphene sheets were quite evenly dispersed in the solvent. This suspension was stable without noticeable sediments even after being shelved for one month. The whole experimental processes lasted only one day and were quite straightforward to implement and control.

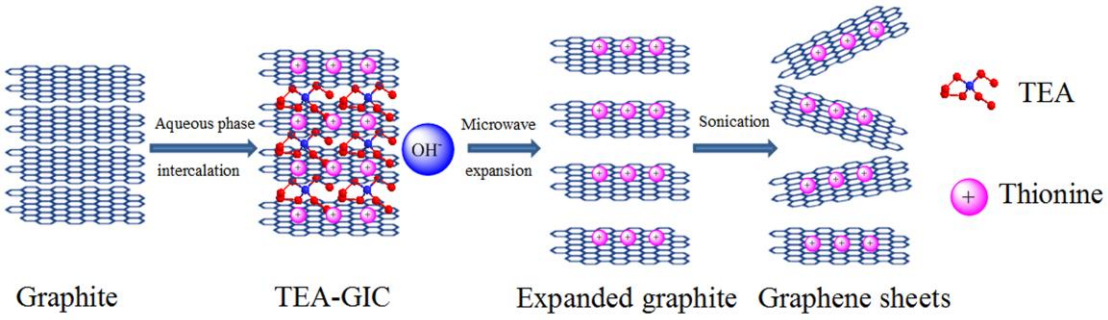

Figure 1. Illustration of experimental procedure for preparation of graphene by liquid phase intercalation and exfoliation of graphite.

3.2 Characterization and mechanism of exfoliation

Figure 2 shows the SEM images of natural graphite, TEA-GIC, and EG. It can be seen that the surface of natural graphite is smooth and compact while the surface of TEA-GIC is tortuous with lamellar structures clearly visible. EG obtained by further microwave irradiation of TEA-GIC presents a paper-like structure and exhibits considerable increase in interlayer spacing compared with natural

graphite and TEA-GIC. The huge expansion from natural graphite to EG will lead to destruction of the long-range periodicity associated with the c-axis of graphite.

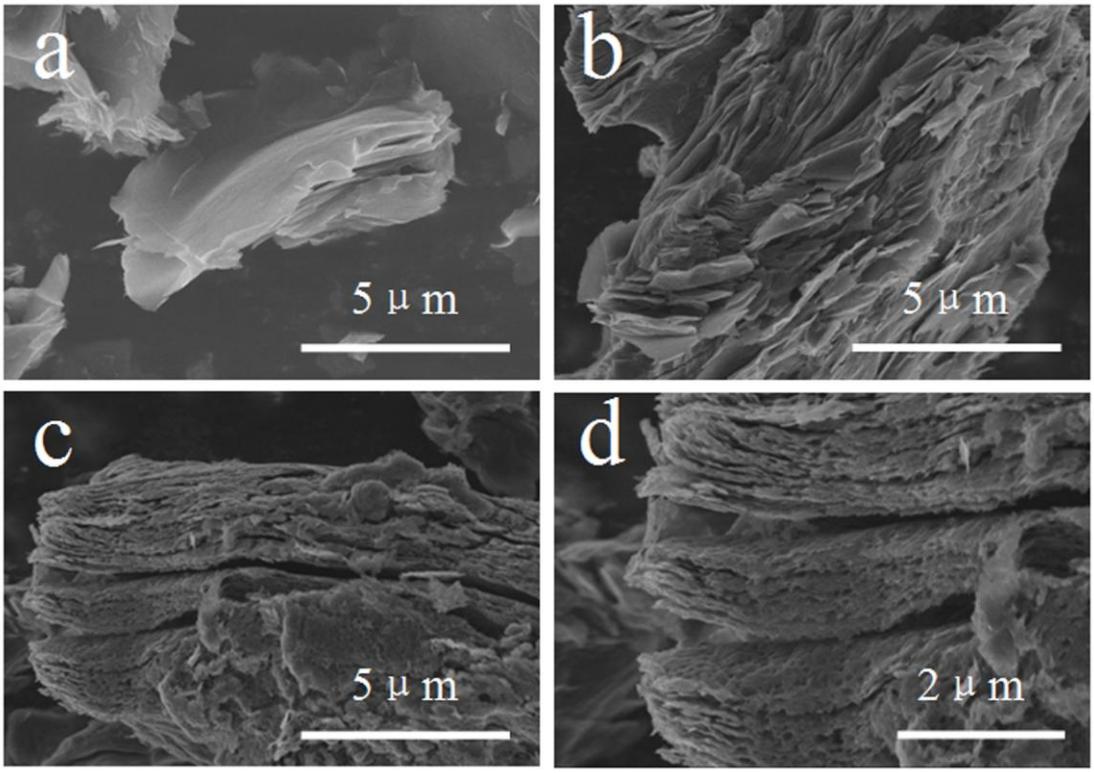

Figure 2. SEM image of (a) natural graphite, (b) TEA-GIC, (c) EG, and (d) the magnified image of (c). Expansion of the precursor graphite is apparent after intercalation with TEA and subsequent treatment by microwave irradiation.

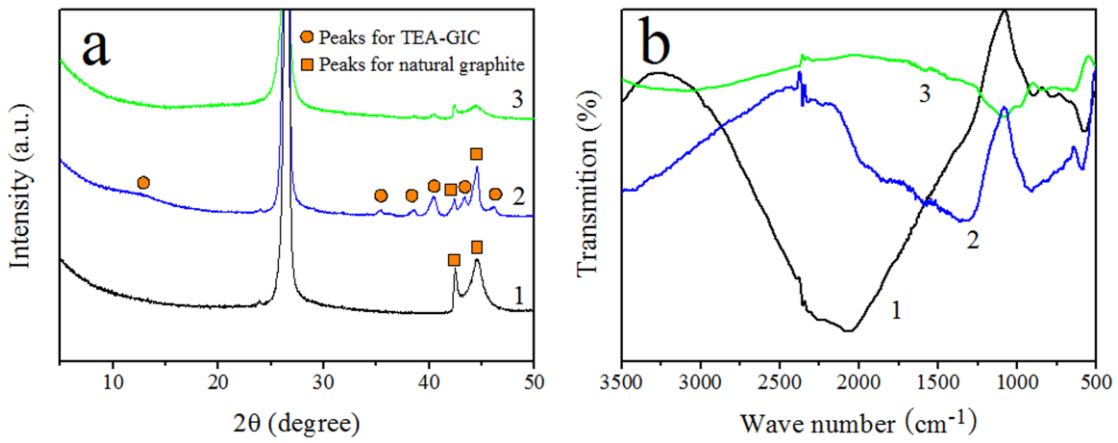

Figure 3. (a) XRD and (b) FTIR spectra of (1) natural graphite, (2) TEA-GIC and (3) EG. The peaks at 2θ = 12.6°, 35.4°, 38.5°, 40.4°, 43.4° and 46.1° in the XRD spectrum of TEA-GIC and the decrease of the intensity or disappearance of these peaks in the spectrum of EG along with the peaks at 1363 and 908 cm^{-1} in the FTIR spectrum of TEA-GIC and their disappearance in the spectrum of EG indicate the insertion and decomposition of TEA in the graphite structure.

Powder XRD patterns of natural graphite, TEA-GIC, and EG are displayed in Figure 3a. A peak related to the periodic lamellar structure of graphite at $2\theta = 26.4°$ and two peaks associated with its in-place crystalline structure at $2\theta = 42.4°$, 44.6° can be seen in all three diffractograms. However, after treatment of natural graphite for aqueous phase intercalation, six additional peaks located at 12.6°, 35.4°, 38.5°, 40.4°, 43.4° and 46.1° showed up, suggesting that TEA cations had successfully entered the interlayer space of natural graphite, which resulted in a change of the lamellar structure in the c-axis direction and also changes of in-plane crystalline structure due to the interaction of TEA with carbon atoms. After microwave treatment of TEA-GIC, the peaks located at 12.6°, 43.4°, 46.1° disappeared and the intensities of the peaks located at 35.4°, 38.5°, 40.4° decreased significantly. This result is attributed to the structural changes in which the TEA cations decomposed under microwave irradiation as expected. Figure 3b displays the FTIR spectra of natural graphite, TEA-GIC, and EG. The peaks at 1363 and 908 cm^{-1} in the spectrum of TEA-GIC are attributed to the shear vibration of $-CH_3$ and stretching vibration of C-N, respectively. The occurrence of these two peaks in the spectrum of TEA-GIC and their disappearance in the spectrum of EG further confirmed the insertion and decomposition of TEA in the graphite structure. It was reported that the TEA cations preferred to interact with the hydroxyl groups on the edges of graphite particles as a consequence of dipole-dipole interactions and may enter graphite galleries due to the cation-π electrostatic interactions [24,25]. Therefore, we believe, under the experimental conditions of this study where intensive sonication was applied to facilitate the vibration of graphite layers, the TEA cations entered successfully the interlayer space of graphite. On the other hand, it was reported that thionin cation was a good stabilizer for graphene dispersion due to its amphiphilic structure, abundance of charge, and strong π-π interaction with graphene [26]. In our experiment, we also used thionin cation to stabilize TEA-GIC and the obtained graphene suspension. The decomposition of TEA under microwave irradiation can be described by the Hofmann and β elimination reactions [27]:

$$Et_4N^+OH^- \longrightarrow C_2H_4 + Et_3N + H_2O \quad (1)$$

$$Et_3N \longrightarrow C_2H_4 + Et_2NH \quad (2)$$

$$Et_2NH \longrightarrow C_2H_4 + EtNH_2 \quad (3)$$

where Et refers to the ethyl group. These reactions were usually carried out under heating (100-200 °C) for two hours. However, under microwave irradiation, they can be shortened to a few minutes [28]. From the above chemical reactions, we can see that gaseous species including C_2H_4 and $EtNH_2$ are produced during the decomposition of TEA. The release of these gaseous species in graphite galleries will lead to huge expansion of graphite layers. This is why graphene sheets can be obtained by mild sonication of EG in organic solvent.

3.3 Morphology of graphene sheets and graphene films

Figure 4a and 4b show the AFM images of a graphene sheet deposited on mica substrate by dip-coating along with a height profile and the histogram of layer numbers of graphene sheets

measured from AFM images, respectively. The thickness of the graphene sheets is about 1 nm on average, calculated from the height difference between the surface of graphene and that of the substrate. This thickness is consistent with triple-layer graphene [29]. By random sampling of thirty graphene sheets, we estimated that 70% of the graphene sheets were comprised of triple-layer graphene, indicating successful synthesis of few-layer graphene of uniform thickness using our method. We also prepared graphene films by filtration. Figure 4c and 4d show the top-view and cross-sectional SEM images of a graphene film, respectively. It can be seen from Figure 4c that the graphene sheets have a uniform lamellar structure with lateral dimensions typically larger than 1 μm. After filtration, the graphene sheets can form paper-like films with which we are exploring their applications in supercapacitors.

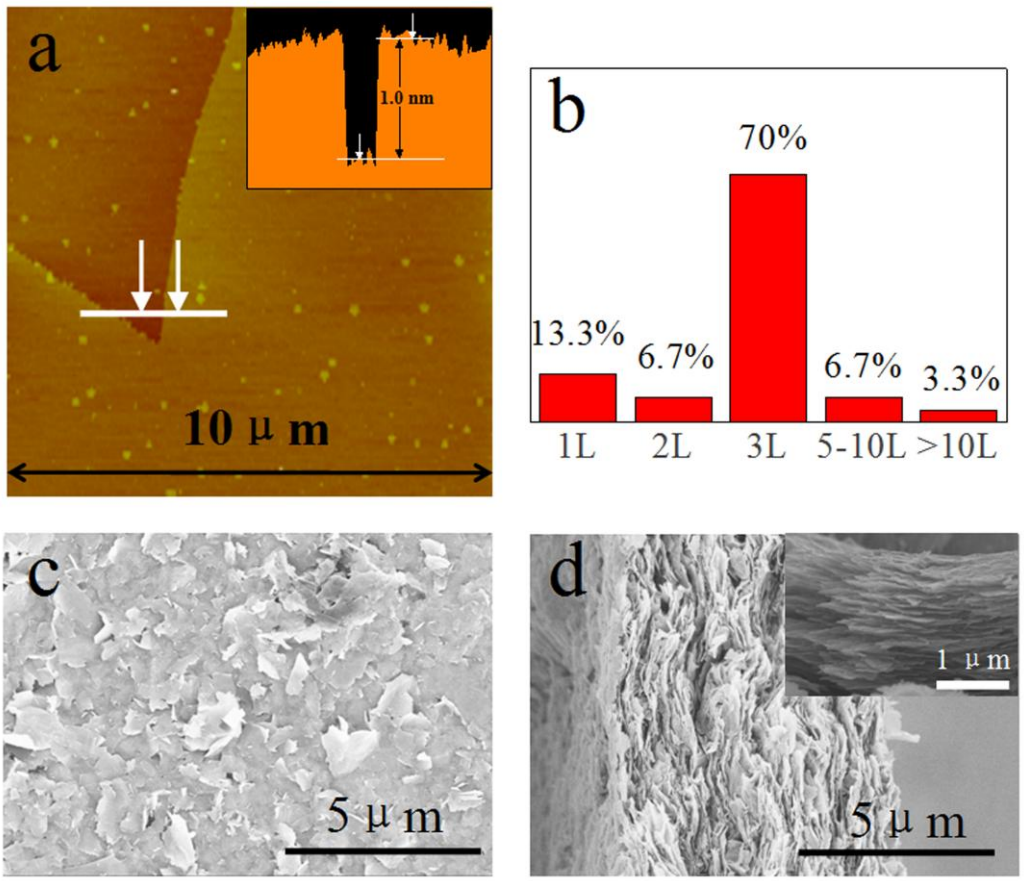

Figure 4. (a) AFM image of a typical graphene sheet. Inset shows the height profile acquired along the line marked in the AFM image. (b) Distribution of graphene layer numbers obtained from AFM analysis of thirty graphene sheets. (c) Top-view SEM image of graphene film. (d) Cross-sectional SEM image of graphene film. The inset is its magnified image.

3.4 Structure and electronic properties of graphene sheets

To examine the number of defects and oxygen functional groups in graphene sheets, Raman and XPS measurement were conducted. There are two peaks in the Raman spectrum of graphene in the range of 1200-1700 cm^{-1}, typically at around 1350 (D peak) and 1560 cm^{-1} (G peak), respectively. The

D peak is ascribed to structural imperfections while the G peak is related to the sp^2 bonded carbon atoms [30]. Therefore, the ratio between the intensity of the D (I_D) and G peaks (I_G) is often used to estimate the number of defects in graphene [23,31,32]. Figure 5a shows a Raman spectrum of graphene film using a 532 nm laser. The intensity ratio, $I_G/I_D \approx 3$ which is several times larger than that of reduced graphene oxide [15], indicates that the concentration of defects is relatively low in our sample. Besides, it was reported that higher disorder in graphite material would lead to a broader G peak [33]. Since the G peak of the graphene is quite sharp, a low concentration of defects in our graphene is therefore confirmed. In addition, the occurrence of the D band may be ascribed to the edge effect of the graphene sheets in the film, not necessarily all due to the defects in graphene [34]. The wide scanning XPS spectrum and its C 1s, S 2p peaks are shown in Figure 5b. The emergence of the S 2p peak indicates that thionin cations are adsorbed on the graphene surface as stabilizer since they are the only sulfur-containing chemical agent in our system. The sharpness of the C 1s peak, indicative of low content of functional groups, demonstrates that the film is mainly composed of pristine graphene.

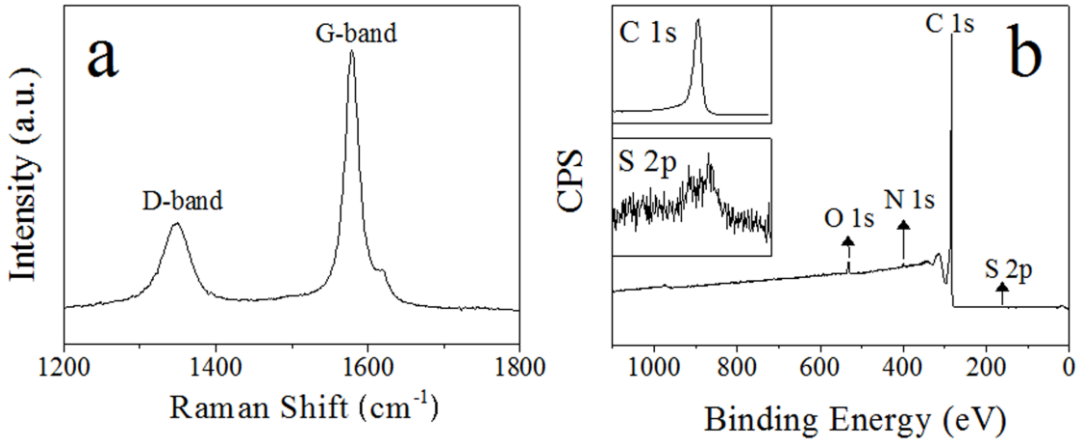

Figure 5. (a) Raman spectrum and (b) XPS spectrum of graphene film. The high intensity ratio I_G/I_D and the sharpness of C 1s peak indicate few defects and little oxidation in the graphene. The emergence of the S 2p peak demonstrates that thionin cations are adsorbed on the graphene surface as stabilizer.

Table 1 lists the weight percentages of all elements present in the sample. The negligible oxygen content along with the high carbon content further confirms that few functional groups exist in our sample. The Raman and XPS data discussed above therefore indicate that our method does not introduce significant structural defects or functional groups to the graphene.

Table 1. Atomic weight percentages from elemental analysis of XPS spectrum.

Samples	C[wt%]	O[wt%]	N[wt%]	Cl[wt%]	S[wt]%
Graphene	96.07	2.58	0.86	0.19	0.29

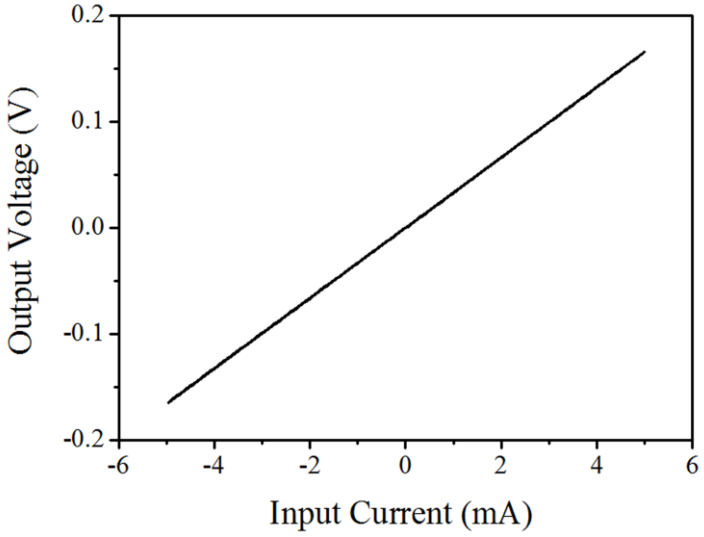

Figure 6. I-V plot of graphene film obtained by PPMS. The resistance of the film is 33.14 Ω, which leads to an electrical conductivity of 4990 ± 710 S/m for the grapheme film.

Table 2. Parameters for calculation of the electrical conductivity of graphene film

Parameters	*L* (mm)	*R* (Ω)	*W* (mm)	*D* (μm)
Value	3.79	33.14	3.34	7±1

To perform measurement of electrical conductivity, the graphene film was cut into a smaller piece with 3.14 × 8.00 mm^2 in dimensions. After fabrication of four electrodes using platinum wires at two sides of the film, of which two electrodes were used to input linearly changing direct current and another two electrodes were used to detect the output voltage, the I-V plot of the film was obtained using PPMS as shown in Figure 6. From this plot, the electrical conductivity of the graphene film was calculated to be 4990 ± 710 S/m according to the following equation:

$$\sigma = L / RWD$$

where *L* is the distance between the two electrodes outputting the voltage, *R* is the resistance obtained from the slope of the I-V plot, and *W* and *D* are the width and thickness of the graphene film, respectively. The values of *L*, *R*, *W* and *D* are given in Table 2. It should be noted that the electrical conductivity is comparable to that obtained by liquid-phase exfoliation of natural graphite [17]. Such a high electrical conductivity is attributed to the fact that few oxidation reactions and little destruction to the graphene occurred in our method of preparation and process of graphene.

4. CONCLUSIONS

Few-layer graphene has been obtained by liquid-phase exfoliation of TEA-GIC which was prepared by high-power tip-sonication of graphite in TEA aqueous solution. This method is easy to

implement with a single-cycle yield of 5%. About 70% of the obtained graphene is about 1 nm in thickness. As no oxidation reactions and little destruction occurred, the obtained graphene has few defects and functional groups. This property makes the graphene possess a high electrical conductivity of about 5000 S m^{-1}.

ACKNOWLEDGMENT
Jie Tang wishes to thank the JST ALCA Program, Japan, for financial support.

References

1. A.K. Geim and K.S. Novoselov, *Nature Mater*., 6 (2007) 183.
2. Y.W. Zhu, S. Murali, W.W. Cai, X.S. Li, J.W. Suk, J.R. Potts and R.S. Ruoff, *Adv. Mater*., 22 (2010) 3906.
3. M.J. Allen, V.C. Tung and R.B. Kaner, *Chem. Rev*., 110 (2010) 132.
4. F. Schwierz, *Nature Nanotechnol*., 5 (2010) 487.
5. P. Avouris, Z.H. Chen and V. Perebeinos, *Nature Nanotechnol*., 2 (2007) 605.
6. M. Burghard, H. Klauk and K. Kern, *Adv. Mater*., 21 (2009) 2586.
7. S. Roth and H.J. Park, *Chem. Soc. Rev*., 39 (2010) 2477.
8. F. Bonaccorso, Z. Sun, T. Hason and A.C. Ferrari, *Nature Photonics*, 4 (2010) 611.
9. M.H. Liang, B. Luo and L.J. Zhi, *Inter. J. Energy Res*., 33 (2009) 1161.
10. F. Han, A.H. Lu and C.W. Li, *Prog. Chem*., 24 (2012) 2443.
11. J. Liu, Y.H. Xue, M. Zhang and L.M. Dai, *MRS Bull*., 37 (2012) 1265.
12. L.L. Zhang, R. Zhou and X.S. Zhao, *J. Mater. Chem*., 20 (2010) 5983.
13. N.M.R. Peres, F. Guinea and A.H.C. Neto, *Phys. Rev*., B 73 (2006) 125411.
14. Y. Xu, H. Bai, G. Lu, C. Li and G. Shi, *J. Am. Chem. Soc*., 130 (2008) 5856.
15. S. Stankovich, D.A. Dikin, R.D. Piner, K.A. Kohlhaas, A. Kleinhammes A, Y.Y. Jia, Y. Wu, S.T. Nguyen and R.S. Ruoff, *Carbon*, 45 (2007) 1558.
16. S. Park and R.S. Ruoff, *Nature Nanotechnol*., 4 (2009) 217.
17. Y. Hernandez , V. Nicolosi, M. Lotya, F.M. Blighe, Z. Sun, S. De, T.T. McGovern, B. Holland, M. Byrne, Y.K. Gun'ko, J.J. Boland, P. Nuraj, G. Duesberg, S. Krishnamurthy, R. Goodhue, J. Hutchison, V. Scardaci, A.C. Ferrari and J.N. Coleman, *Nature Nanotechnol*., 3 (2008) 563.
18. L.M. Virculis, J.J. Mack, O.M. Mayer, H.T. Hahn and R.B. Kaner, *J. Mater. Chem*., 15 (2005) 974.
19. J.H. Lee, D.W. Shin, V.G. Makotchenko, A.S. Nazarov, V.E. Fedorov, Y.H. Kim, J.Y. Choi, J.M. Kim and J.B. Yoo, *Adv. Chem*., 21 (2009) 4383.
20. W.T. Gu, W. Zhang, X.M. Li, H.W. Zhu, J.Q. Wei, Z. Li, Q. Shu, C. Wang, K.L. Wang, W. Shen, F.Y. Kang and D.H. Wu, *J. Mater. Chem*., 19 (2009) 3367.
21. E.H.L. Falcao, R.G. Blair, J.J. Mack, L.M. Viculis, C.W. Kwon, M. Bendikov, R.B. Kaner and B.S. Dunn, *Carbon*, 45 (2007) 1367.
22. W. Qian, R. Hao, Y.L. Hou, Y. Tian, C.M. Shen, H.J. Gao and X.L. Liang, *Nano Res*., 2 (2009) 706.
23. U. Khan, A. O'Neill, M. Lotya, S. De and J.N. Coleman, *Small*, 6 (2010) 864.
24. Z. Liu, Z.M. Wang, X. Yang and K. Ooi, *Langmuir*, 18 (2002) 4926.
25. P.K. Ang, S. Wang, Q.L. Bao, J.T. L. Thong and K.P. Loh, *ACS Nano*, 3 (2009) 3587.
26. C. Chen, W.T. Zhai, D.D. Lu, H.B. Zhang and W.G. Zheng, *Mater. Res. Bull*., 46 (2011) 583.
27. E. Bourgeat-Lami, F.F. Di Renzo, P.H. Mutin and T. Des Courieres, *J. Phys. Chem*., 96 (1992) 3807.
28. K.D. Raner, C.R. Strauss, R.W. Trainor and J.S. Thorn, *J. Org. Chem*., 60 (1995) 2456.

29. P. Nems-Incze, Z. Osváth, K. Kamarás, L.P. Biró, *Carbon*, 46 (2008) 1435.
30. Z.H. Ni, Y.Y. Wang, T. Yu and Z.X. Shen, *Nano Res*., 1 (2008) 273.
31. G.X. Wang, B. Wang, J. Park, Y. Wang, B. Sun and J. Yao, *Carbon*, 47 (2009) 3242.
32. W.C. Oh and F.J. Zhang, *Asian J. Chem*., 23 (2011) 875.
33. K.N. Kudin, B. Ozbas, H.C. Schniepp, R.K. Prud'homme, I.A. Aksay and R. Car, *Nano Lett*., 8 (2008) 36.
34. A.C. Ferrari, J.C. Meyer, V. Scardaci, C. Casiraghi, M. Lazzeri, F. Mavri, S. Piscanec, D. Jiang, K.S. Novoselov, S. Roth and A.K. Geim, *Phys. Rev. Lett*., 97 (2006) 187401.